

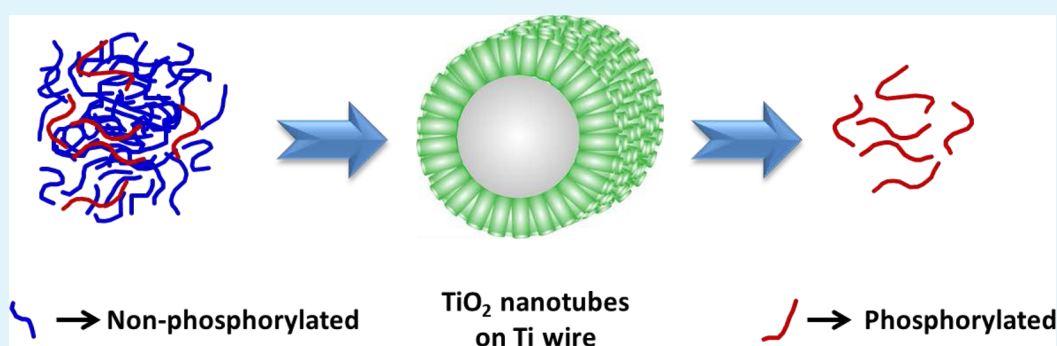
Phosphopeptide Separation Using Radially Aligned Titania Nanotubes on Titanium Wire

Aruna B. Wijeratne,[†] Dharshana N. Wijesundera,[‡] Maggie Paulose,[§] Ivy Belinda Ahiabu,[§] Wei-Kan Chu,[‡] Oomman K. Varghese,^{*,§} and Kenneth D. Greis^{*,†}

[†]Department of Cancer Biology, The University of Cincinnati College of Medicine, Cincinnati, Ohio 45267, United States

[‡]Department of Physics and Texas Center for Super Conductivity (TcSUH) and [§]Nanomaterials and Devices Laboratory, Department of Physics, University of Houston, Houston, Texas 77204, United States

S Supporting Information



ABSTRACT: Phosphoproteomic analysis offers a unique view of cellular function and regulation in biological systems by providing global measures of a key cellular regulator in the form of protein phosphorylation. Understanding the phosphorylation changes between normal and diseased cells or tissues offers a window into the mechanism of disease and thus potential targets for therapeutic intervention. A key step in these studies is the enrichment of phosphorylated peptides that are typically separated and analyzed by using liquid chromatography mass spectrometry. The mesoporous titania beads/particles (e.g., Titansphere TiO₂ beads from GL Sciences Inc., Japan) that are widely used for phosphopeptide enrichment are expensive and offer very limited opportunities for further performance improvement. Titania nanotube arrays have shown promising characteristics for phosphopeptide separation. Here we report a proof-of-concept study to evaluate the efficacy of nanotubes on Ti-wire for phosphoproteomics research. We used titania nanotubes radially grown on titanium wires as well as the commercial beads to separate phosphopeptides generated from mouse liver complex tissue extracts. Our studies revealed that the nanotubes on metal wire provide comparable efficacy for enrichment of phosphopeptides and offer an ease of use advantage versus mesoporous beads, thus having the potential to become a low cost and more practical material/methodology for phosphopeptide enrichment in biological studies.

KEYWORDS: phosphoproteomics, titanium dioxide, nanotube array, phosphopeptide separation, chromatography, mesoporous

1. INTRODUCTION

Reversible protein phosphorylation is a central regulatory mechanism for normal biological function and cellular homeostasis, while dysregulation of phosphorylation can lead to the initiation and propagation of a variety of diseases.^{1,2} As such, studies aimed at understanding the dynamics of phosphorylation on a global scale in control versus disease conditions have come to the forefront of biological research as the research community attempts to understand the underlying cellular mechanisms of disease with the goal of providing new targets for therapeutic intervention. The global study of cellular phosphorylation of proteins, commonly called phosphoproteomics, is typically done by first digesting the proteins into specific peptides, followed by separation, identification, and quantification of the peptides by liquid chromatography coupled with mass spectrometry (LC-MS).^{3,4} The success of

these methods is highly dependent on the investigator's ability to effectively separate or enrich the phosphopeptides from nonphosphorylated peptides. This enrichment is required for several reasons: (1) many phosphorylated proteins are in low abundance compared to the total cellular protein, and hence, their detection from a complex cellular mixture may be compromised due to the dynamic range of total proteins available; (2) phosphorylation site occupancy on many proteins is often at a low stoichiometry (typically <5% but for phosphotyrosine it can be less than 0.1%) thus further diminishing the amount of phosphorylated peptide available for detection; (3) when using electrospray ionization (ESI)

Received: January 27, 2015

Accepted: May 5, 2015

Published: May 5, 2015

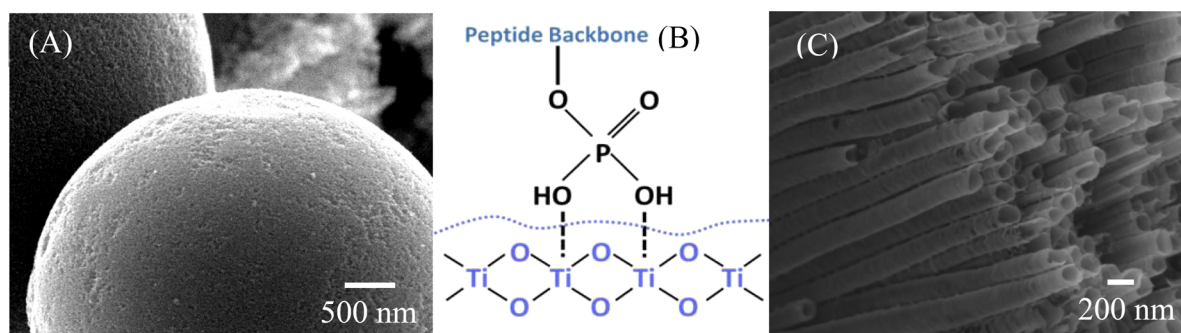


Figure 1. SEM image of second generation Titansphere TiO₂ Bulk Material-beads obtained from GL Sciences Inc. Japan.¹⁸ The image illustrates the spherical morphology associated with the beads and their porosity. (B) Bidentate interaction of the phosphopeptide with TiO₂.³⁴ (C) Tilted surface view of the TiO₂ nanotube array revealing the ordered porous architecture.

mass spectrometry, phosphopeptides are prone to ionization suppression in the positive ion mode when they are analyzed simultaneously with nonphosphorylated peptides.^{4,5} Given these challenges, the research community continually strives to develop ways to enhance the detection and quantification of the phosphopeptides.

For phosphopeptide enrichment, a variety of metal chelation and metal oxide affinity materials have shown great promise^{6,7} with titanium dioxide (TiO₂) having emerged as the most popular and widely utilized material.^{8–17} This is due in part to the observed robustness and tolerance of TiO₂ toward various reagents, including buffers, salts, and detergents that are commonly used in biological protein preparations.¹³ This metal oxide, either as spherical porous beads¹⁴ or nanocomposite material in powder form,¹⁵ has demonstrated high efficacy for enrichment via capture of the phosphate group of phosphopeptides in a bridging bidentate configuration between proximal TiO₂ groups on the surface of the material.¹⁴ This interaction can be disrupted by high pH elution, and the enriched phosphopeptides can be further evaluated by mass spectrometry.

While TiO₂ enrichment represents one of the currently best available options for phosphopeptide enrichment, it is not without some significant limitations. First, due to the similar chemical structure of peptides containing aspartic or glutamic acids compared to phosphorylated peptides, considerable levels of acidic peptides are also captured by TiO₂. This can be partially overcome by including competing additives (e.g., dihydroxybenzoic acid, glycolic acid) in the binding and wash buffers to compete away some of the acidic peptide binding.^{12–14} Second, optimization of the amount of TiO₂ material needed for a given protein extraction has proven to be challenging based on reports indicating that the efficiency of phosphopeptide capture is highly dependent on having the correct ratio of TiO₂ to peptides.¹⁹ This means that the optimum ratio must be determined empirically for each sample set, thus having a significant impact on the general utility of the method. Another significant challenge is the practical handling of the currently available materials. Typical use of these materials for phosphopeptide enrichments involves preparation of a slurry suspension of the “powdery” material in an appropriate buffer.^{12–16} The material is then packed into micro columns^{12,14,17,18} or used as solid phase media in optimized/controlled amounts to capture phosphopeptides.^{16,19} Practical considerations such as weighing out the desired amount of material, transfer of precise amounts from the slurry suspension into each sample, and removing the

material after eluting the phosphopeptides all add to the variability between experiments. Finally, the most commonly used material for these studies (Titansphere TiO₂ Bulk Material-beads¹⁸) is only available in one format as highly porous and spherical beads (Figure 1A) with limited options for further optimization for phosphopeptide enrichment. Consequently, investigation of TiO₂ materials in another format may provide significant advantages in ease of use, optimization, and reproducibility of phosphopeptide enrichment strategies.

In recent years, titania nanotube arrays grown by anodic oxidation have emerged as a useful material for a wide variety of applications including gas sensing, dye sensitized solar cells, hydrogen generation by water photoelectrolysis, organic electronics, microfluidics, molecular filtration, drug delivery, and tissue engineering.^{20–27} Since they have a highly ordered nanostructure with enormous surface area, titania nanotube arrays have also begun to show some promise for phosphopeptide separation.^{28,29} For example, Lo et al.²⁸ have reported 250-nm-long nanotube arrays, fabricated by anodizing titanium foils in aqueous hydrofluoric acid electrolyte, as substrate for surface-assisted laser desorption/ionization mass spectrometry (SALDI MS). They used a tryptic digest of β -casein for the study and illustrated that phosphopeptides could be selectively trapped on titania nanotubes. In addition, titania thin nanotube array films prepared on glass and patterned in ‘S’ shapes have recently been reported by Min et al.²⁹ for phosphopeptide enrichment and found to be useful for differential expression analysis of endogenous phosphopeptides between ovarian cancer patients and healthy women. Despite these different studies, concerted efforts to explore the potential of these materials as alternative and perhaps superior options to the current standard materials used for phosphoproteomic research are very limited in the literature. To expand the understanding of these materials, the current study provides a proof-of-concept evaluation of radially aligned titanium dioxide nanotubes (TNTs) on titanium wire (Ti-wire).

While fabrication of TNT arrays using anodic oxidation is known for its simplicity, cost effectiveness, and industrial viability,^{20–22,30,31} the primary advantage of using TNTs on titanium wire for phosphopeptide enrichment is that the surface area can be readily standardized in terms of the length of the wire. One can thus cut the wire into desired lengths to precisely and reproducibly generate the required active surface area for a given phosphopeptide enrichment method. Moreover, the nanotubes grown on wires do not mix into the solution or make colloidal dispersions, and hence, in contrast to commonly

used Titansphere TiO₂ beads, nanotubes-on-wire architecture carries the added benefit of avoiding practical difficulties in separating beads from the solvent medium after elution of the phosphopeptides. In this study, we evaluated the efficacy of radially aligned titania nanotubes grown on titanium wire in comparison with the widely used, but expensive Titansphere TiO₂ Bulk Material-beads¹⁸ in order to understand if this material could be a low cost alternative for practical use in phosphoproteomic research. Our experiments indicated that radially aligned TNTs grown on Ti-wire surfaces are highly suitable for isolating phosphopeptides. Peptides generated from a standard phosphoprotein (α -casein) and mouse liver complex tissue extracts were used in the study. The architecture performed at a comparable level to the standard Titansphere TiO₂ Bulk Material-beads, while this medium possesses other desirable attributes mentioned above that provide ample room for further improvements.

2. EXPERIMENTAL SECTION

2.1. Materials. Guanidine:hydrogen chloride (GHCl), ammonium bicarbonate (NH₄HCO₃), phosphatase inhibitor cocktail 2 (cat. no. P5726), dithiothreitol (DTT), iodoacetamide (IAA), formic acid (HCOOH, FA), trifluoroacetic acid (TFA), α -casein from bovine milk (cat. no. C6780, *as*-casein minimum 70%), acetonitrile (CHROMASOLV, for HPLC, gradient-grade, >99.9%), water (CHROMASOLV-Plus, for HPLC), α -cyano-4-hydroxycinnamic acid (CHCA), and glycolic acid were purchased from Sigma-Aldrich (St. Louis, MO). For proteomics sample preparation work flow, deionized water was obtained from an in-house Milli-Q system (Millipore, Bedford, MA). All centrifugation steps were completed in an IEC Micromax RF microfuge at 14 600 RCF (Relative Centrifugal Force). Modified trypsin was obtained from Promega (Madison, WI). Oligo R3 reversed-phase material was obtained from Applied Biosystems (Foster City, CA). For the packing of Oligo R3 reversed phase material, Bioselect extraction columns (reversed phase C4) were obtained from GRACE-VYDAC (W.R. Grace & Co., Deerfield, IL). For TiO₂-chromatography using "beads", Titansphere TiO₂-beads were obtained from GL Sciences Inc. For TiO₂-chromatography using "wires", titanium wire of diameter 0.25 mm (99.7% pure) purchased from Sigma-Aldrich was used. The electrolyte for anodization of the wire consisted of ammonium fluoride (ACS reagent, 98%, Sigma-Aldrich) and ethylene glycol (anhydrous, 99.8%, Sigma-Aldrich) and deionized water.

Ammonium hydroxide (trace-metal grade, assay: 20–22% as NH₃) was obtained from Fisher Scientific (Hampton, NJ) for phosphopeptide elution during TiO₂-chromatography. Whole mouse liver samples were Dounce homogenized in the presence of both protease and phosphatase inhibitor cocktails all as described previously.³² Protein concentrations were also determined using NI (Non-Interfering) Protein Assay-Kit purchased from G-BIOSCIENCES.

2.2. Preparation and Characterization of TiO₂ Nanotubes on Ti Wire. The Ti wire (diameter ~0.25 mm) was cut into ~25-mm-length and degreased by sonication in acetone and then in isopropanol. The degreased wires were again cleaned sequentially in water and Micro-90, isopropanol, and acetone and dried with nitrogen gas. Anodization was conducted at room temperature in an electrolyte consisting of 0.3 wt % NH₄F, 2 vol % H₂O in ethylene glycol. The titanium wire was used as anode and platinum foil as cathode. The anodization was performed for 4 h with 60 V applied between the electrodes. The anodized wires were washed and sonicated in isopropanol to remove debris formed on the surface of the nanotubes during the anodization process. The cleaned samples were annealed at 530 °C in oxygen for 3 h.³³

The morphology of the nanotubes on Ti wire was studied using a field emission scanning electron microscope (FESEM; LEO 1512S). The crystal structure was identified using a high resolution transmission electron microscope (HRTEM; JEOL 2010) and glancing angle X-ray diffractometer (GAXRD; Rigaku, Smartlab, Cu

K α). A single wire coated with nanotubes was used for GAXRD measurements. The incident angle was 3.0°. The X-ray photoelectron spectroscopy (XPS; Physical Electronics, model 5700) was used to determine the composition of the samples.

2.3. Trypsin Digestion. Precisely as reported previously,¹⁶ 500 μ g aliquots of protein were precipitated with 8 volumes of cold acetone (–20 °C) in 1.5 mL Eppendorf tubes. After centrifugation (14 600 RCF, 5 min), supernatants were discarded and pellets were washed three times using –20 °C acetone (100 μ L for each wash). Sample tubes were then kept open in a fume-hood for 2 min to ensure any residual acetone vaporization. The pellets were reconstituted in 3 M Guanidine:HCl in 100 mM NH₄HCO₃ (90 μ L) containing phosphatase inhibitor cocktail (2 μ L). The solutions were subsequently reduced with DTT (1 mM final concentration, incubated at 37 °C, for 45 min) and then alkylated with iodoacetamide (5.5 mM final concentration, incubated at 37 °C, for 30 min). The solutions were finally diluted with ddH₂O to 1 mL before trypsin-based digestion. 100 μ g of modified trypsin was dissolved in 300 μ L of 0.1 M NH₄HCO₃, and 10 μ g aliquots were added into each 500 μ g protein sample (i.e., 1:50 weight ratio). Samples were then incubated overnight at 37 °C, and the digestion was quenched by adding 20 μ L of formic acid (to bring the pH of solutions to less than 5). After centrifugation, the supernatants were recovered for further processing. Similarly, 500 μ g of bovine α -casein was subjected to trypsin digestion for qualitative comparison of phosphopeptide separation using Titansphere¹⁸ TiO₂ Bulk Material-beads ("beads") and Ti-wire surface grown with TiO₂ nanotubes ("wires").

2.4. Desalting of Tryptic Peptides Using OligoR3 Beads. Oligo R3 reversed-phase material was dispersed in ACN/H₂O/TFA 70/29.9/0.1 (v/v/v) to make a 60 mg/mL slurry as previously described,^{16,17} and divided into 500 μ L aliquots each containing 30 mg of Oligo R3 beads in 1.5 mL Eppendorf tubes. The beads prepared for peptide desalting by sequential vortex, spin, and removal of the supernatant followed by two wash steps using 200 μ L of 0.1% TFA in Milli-QH₂O. Peptide solutions were added onto washed Oligo R3 beads and incubated for 30 min at room temperature using end-over-end rotation. GRACE-VYDAC BIOSELECT-C4 columns (cat. no. 214SPE1000) were adapted onto an extraction manifold (Waters Manifold, Massachusetts, USA), washed sequentially with (1) ACN (500 μ L), (2) ACN/TFA/H₂O 70/0.1/29.9 (v/v/v, 200 μ L), (3) 0.1% TFA (500 μ L), and (4) dd H₂O (500 μ L), and then packed with peptide-bound Oligo R3 beads by a gentle application of vacuum into the extraction manifold vacuum chamber. Subsequently, the peptide-bound beads were washed with 500 μ L ddH₂O and eluted by sequentially passing 200 μ L of ACN/TFA/H₂O 90/0.1/9.9 (v/v/v) for one time and then 200 μ L of ACN/TFA/H₂O 70/0.1/29.9 (v/v/v) for two times. All elution fractions were collected into 1.5 mL Eppendorf tubes. Prior to TiO₂-chromatography, these elution fractions were subjected to vacuum centrifugation for complete dryness.

2.5. Separation of Phosphopeptides Using TiO₂-Chromatography. Phosphopeptide separation of the peptide mixtures was carried out using an optimized strategy adapted from previous reports,^{16,17,19} and was performed in triplicate using identical protein samples for each TiO₂-chromatographic method. In using the "beads" for phosphopeptide separation, briefly for each replicate, Titansphere TiO₂ beads were dispersed in ACN/H₂O/TFA 80/15/5 (v/v/v) to make a 100 μ g/ μ L slurry and then divided into 5 μ L aliquots each containing 500 μ g of TiO₂ beads in 0.5 mL Eppendorf tubes. Each vial was subjected to a vortex and spin with supernatants discarded, followed by 2 additional wash steps using 200 μ L of 0.1% TFA in Milli-QH₂O. Dried peptide mixtures (500 μ g) were reconstituted in 200 μ L of 1 M glycolic acid in ACN/H₂O/TFA 80/15/5 (v/v/v), and loaded onto the prewashed Titansphere TiO₂-beads. The peptides were allowed to interact with the TiO₂ for 30 min at room temperature using end-over-end rotation. The TiO₂ beads were then sequentially washed with 400 μ L ACN/H₂O/TFA 80/15/5 (v/v/v) with a spin and removal of the supernatant followed by an additional 400 μ L wash with the same solvent. Finally the phosphopeptides captured on the TiO₂-beads were eluted 1 time with 200 μ L of 5%

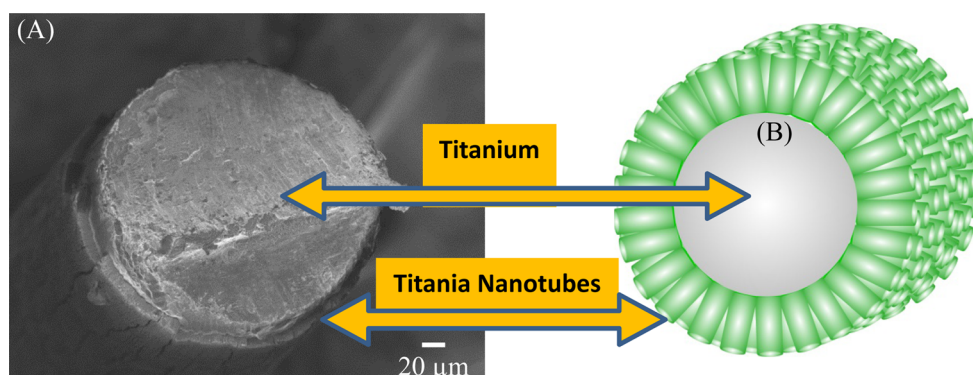


Figure 2. (A) Cross-sectional SEM image of an as-anodized wire sample showing titania nanotube layer (thickness $\sim 15 \mu\text{m}$) covering the titanium wire (diameter $\sim 0.25 \text{ mm}$). (B) Schematic representation to show the orientation of the nanotubes on the surface of the wire substrate (nanotube length and diameter not to scale).

NH_4OH . In using the “wires” for phosphopeptide separation, briefly for each replicate, Ti-wire pieces ($4 \times 0.5 \text{ cm}$, i.e., 2.0 cm in length) grown with TiO_2 nanotubes were placed inside 0.5 mL Eppendorf tubes and subjected to similar washing steps. Following reconstitution of dried peptide mixtures ($500 \mu\text{g}$) in $200 \mu\text{L}$ of 1 M glycolic acid in $\text{ACN}/\text{H}_2\text{O}/\text{TFA}$ $80/15/5$ (v/v/v), peptide mixtures were loaded onto the prewashed Ti-wire pieces grown with TiO_2 nanotubes. TiO_2 “wires” with loaded peptides were then sequentially washed with $400 \mu\text{L}$ $\text{ACN}/\text{H}_2\text{O}/\text{TFA}$ $80/15/5$ (v/v/v) with a spin and removal of the supernatant followed by an additional $400 \mu\text{L}$ wash with the same solvent. Finally the phosphopeptides captured on the TiO_2 “wires” were also eluted 1 time with $200 \mu\text{L}$ of $5\% \text{ NH}_4\text{OH}$. The NH_4OH elution fractions were dried by vacuum centrifugation prior to nanoLC-MS/MS analysis. For the standard phosphopeptide mixture obtained from α -casein trypsin digestion, $2.5 \mu\text{L}$ aliquots of the elution fractions were removed from each sample, desalted by ZipTip(C-18 μ) as described by the manufacturer (Millipore) and evaluated by Matrix-Assisted Laser Desorption Ionization–Time of Flight–Mass Spectrometry (MALDI-TOF-MS) to qualitatively investigate phosphopeptide separation.

2.6. Mass Spectrometry Analysis. MALDI-MS analysis was performed on a 4800 MALDI-TOF/TOF instrument (AB Sciex, Foster City, CA). Mass spectra were obtained in positive ion reflector mode. MALDI-matrix solution was prepared by dissolving α -cyano-4-hydroxy-cinnamic acid (CHCA, 5 mg) in 10 mM ammonium phosphate (monobasic) in $\text{ACN}/\text{FA}/\text{H}_2\text{O}$ $60/0.1/39.9$ (v/v/v, 1 mL). In order to perform MALDI-MS analyses, desalted (using Oligo R3 reversed phase material or ZipTip(C-18 μ)) and isolated peptides in solution ($0.5 \mu\text{L}$) were mixed with MALDI-matrix solution ($1 \mu\text{L}$), and spots were placed on a calibrated MALDI plate.

Nano-LC-MS/MS analyses were performed on a TripleTOF 5600 (ABSciex, Toronto, ON, Canada) coupled to an Eksigent (Dublin, CA) nanoLC.ultra nanoflow system. Dried phosphopeptide samples were reconstituted in $\text{FA}/\text{H}_2\text{O}$ $0.1/99.9$ (v/v) and loaded onto IntegraFrit Trap Column (outer diameter of $360 \mu\text{m}$, inner diameter of 100 , and $25 \mu\text{m}$ packed bed) from New Objective, Inc. (Woburn, MA) at $2 \mu\text{L}/\text{min}$ in $\text{FA}/\text{H}_2\text{O}$ $0.4/99.2$ (v/v) for 10 min to desalt and concentrate the samples. For the chromatographic separation of peptides, the trap-column was switched to align with the analytical column, Acclaim PepMap100 (inner diameter of $75 \mu\text{m}$, length of 15 cm , C18 particle sizes of $3 \mu\text{m}$ and pore sizes of 100 \AA) from Dionex-Thermo Fisher Scientific (Sunnyvale, CA). The peptides were eluted using a varying mobile phase (MP) gradient from 95% phase A ($\text{FA}/\text{H}_2\text{O}$ $0.4/99.6$, v/v) to 40% phase B (FA/ACN $0.4/99.6$, v/v) for 70 min , from 40% phase B to 85% phase B for 5 min and then keeping the same MP-composition for 5 more minutes at $300 \text{ nL}/\text{min}$.

Nano-LC mobile phase was introduced into the mass spectrometer using a NANOSpray III Source (AB Sciex, Toronto, On, Canada). Ion source gas 1 (GS1) was zero grade air while ion source gas 2 (GS2) and curtain gas (CUR) were both nitrogen. The “gas settings” were kept at 7 , 0 , and 25 , respectively, in vendor specified arbitrary units.

Interface heater temperature and ion spray voltage was kept at $150 \text{ }^\circ\text{C}$, and at 2.3 kV . The mass spectrometer method was operated in positive ion mode set to go through 4156 cycles for 90 min , where each cycle consisted of one TOF-MS scan (0.25 s accumulation time, in a 400 to 1600 m/z window) followed by 20 information dependent acquisition (IDA) mode MS/MS-scans on the most intense candidate ions selected from initially performed TOF-MS scan during each cycle, having a minimum of 150 counts. Each product ion scan was operated under vendor specified high-sensitivity mode with an accumulation time of 0.05 s and a mass tolerance of 50 mDa . Former MS/MS-subjected candidate ions were excluded for 10 s after its first occurrence, and data were recorded using Analyst-TF (1.5.1) software.

Identification of Phosphopeptides. The nano-LC-MS/MS data (*.wiff file) from the enriched phosphopeptides were analyzed for peptide/protein identification using ProteinPilot software (version 4.2, revision 1297) that integrates the Paragon algorithm, searched against a SwissProt database of *Mus musculus* protein sequences on a local 12-processor server. A custom “sample-type” was selected that specifies variable biological modifications as specified defaults in the ProteinPilot software. The vendor defined phosphorylation emphasis on serine/threonine/tyrosine was also used as a special factor. The resulting *.group files were then used to generate a spreadsheet as a peptide summary report. Only those phosphopeptides identified with a minimum of 95% confidence in identity (calculated by probability algorithms of ProteinPilot software), and phosphorylation as a modification were selected as viable phosphopeptide identifications. Unique phosphopeptides were then selected based on sequence, modifications, and mass to charge ratio (m/z -value) using available software tools on Microsoft Excel. Tools made available by Microsoft Excel were used to determine the number of unique phosphopeptides for each replicate and each TiO_2 -chromatography method employed.

3. RESULTS AND DISCUSSION

3.1. TiO_2 in Phosphopeptide Separation. Figure 1 shows the SEM images of the Titansphere TiO_2 Bulk Material-beads and titania nanotubes on Ti wire on either sides with a schematic representation of bidentate interaction of phosphopeptide with TiO_2 in the middle. Bidentate coordination of hydroxyl groups to positively polarized Ti(IV) on TiO_2 colloidal surface is likely the mode of action that accounts for preferential capture and enrichment of phosphorylated peptides (Figure 1B).^{34–36} Connor and McQuillan first studied the adsorption of phosphate ions on thin films of colloidal TiO_2 using in situ internal reflection infrared spectroscopy.³⁶ They have observed similar Langmuir binding constants for phosphate ions and bidentate ligand species such as oxalate and catechol onto colloidal TiO_2 at low pH (2.3)—inferring bidentate ligation of phosphorylated peptides on to TiO_2 as the mechanism for selective capture of phosphopeptides.

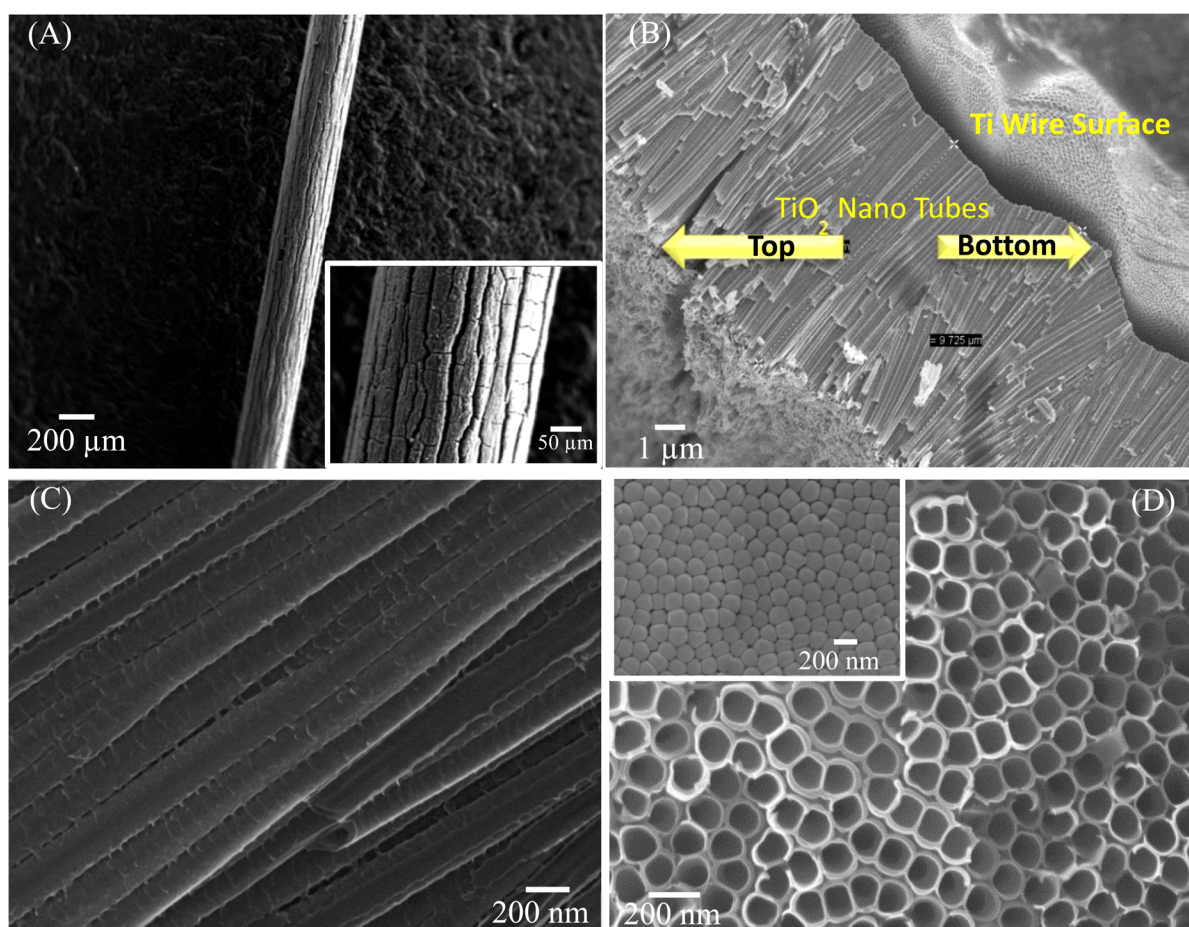


Figure 3. SEM images of titania nanotubes grown on titanium wire substrates. (A) Image of a Ti wire covered with TiO_2 nanotubes. A higher magnification image is shown in the inset. (B) Side view of the nanotubes (length $\sim 10 \mu\text{m}$) attached to the wire substrate. (C) Magnified lateral view of the nanotubes. (D) Top surface of the nanotubes. An image of the bottom surface of the nanotubes detached from the wire substrate is given in the inset.

Although the pore openings in commercially available Titansphere TiO_2 Bulk Material-beads are more or less uniformly distributed (Figure 1A), the pore size (depth and diameter) is randomly distributed, which limits the opportunities to further optimize the surface area to enhance phosphopeptide enrichment. In contrast, TNTs on Ti wire are highly ordered, with definite pore size and distribution as evident from the SEM images in Figures 1–3. The ability to readily control both the length and porosity of TNTs makes them an attractive alternative for further improving how phosphopeptide enrichment is performed in phosphoproteomics profiling workflows. Although titania nanotubes can be grown on various substrates such as titanium, glass, and silicon having different shapes,^{25,29,37,39} the practically useful substrates and architectures are those providing robustness in phosphopeptide enrichment and ease in determining and optimizing the surface area for effective phosphoproteomics profiling. Radially aligned titania nanotubes grown on wire is such an architecture where surface area of nanotubes can be readily standardized in terms of length of the wire so that a user having an idea of the surface area per unit length of the wire can easily cut and use a wire length that provide the desired surface area. Growth of nanotubes on cylindrical shapes such as wires and pipes was reported,^{37–39} but to the best of our knowledge, the utility of these surfaces for phosphopeptide enrichment has not been investigated. Thus, the goal of the present study is to provide

insight on the potential of TNTs on Ti-wire as a viable alternative to Titansphere TiO_2 Bulk Material-beads for phosphopeptide separations.

3.2. Titania Nanotube Arrays on Ti-Wire. In order to understand the phosphopeptide separation efficiency of the titania nanotube arrays relative to the most utilized material in the field, we performed TiO_2 -chromatography in parallel using (1) the most popularly used and commercially available Titansphere TiO_2 Bulk Material-beads as a reference material (“Beads”) and (2) Ti-wire pieces grown with TiO_2 nanotubes (“Wires”), on a standard phosphoprotein, α -casein and also on mouse liver lysates, to illustrate their phosphopeptide separation capacity and their applicability in studying complex biological proteomes, respectively. Surfaces of Ti “wire” pieces were modified with TiO_2 -nanotubes (Figure 2A,B), and the wires were particularly chosen so that they could be readily cut into pieces so that effective surface area can be simply controlled by specific lengths.

Anodization of titanium wires per the conditions given in the experimental section resulted in the growth of highly ordered nanotubes pointing radially outward from the surface. The SEM image of the cross section of a nanotube-covered Ti wire sample (diameter $\sim 0.25 \text{ mm}$) is given in Figure 2A and an expanded view of the nanotubes on the wire surface is schematically represented in Figure 2B. The growth and self-organization of the nanotubes take place during the anodization

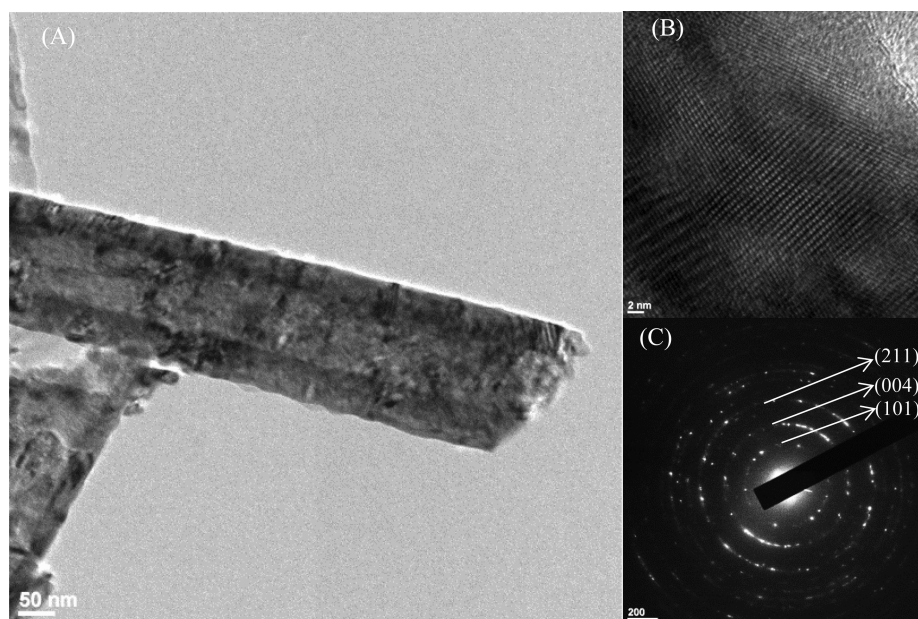


Figure 4. HRTEM image of a nanotube grown on Ti wire (a) and the polycrystalline lattice (b). The SAD pattern showing reflections from titania anatase phase is given in (c).

process and are believed to be due to the interplay between electric field assisted oxidation of titanium metal and chemical dissolution as well as electric field assisted dissolution of the oxide.²³ An alternate model suggests a stress induced displacement of material rather than field assisted dissolution as responsible for the anodic growth of porous structures.^{24,40} Nevertheless, the nanotubes are grown more or less perpendicular to the substrate surface by consuming the metal and converting into oxide regardless of the growth conditions.

The anodization of titanium in organic electrolytes such as ethylene glycol generally produces anodization debris in the form of particles or nanowires or bunched/broken tubes on the surface of the sample. To remove the debris from the surface of the nanotubes, we subjected the wire samples to ultrasonic agitation at 35 kHz as used normally for other substrates. However, the nanotube films peeled during sonication due to the stress at the oxide/metal interface. The problem was eliminated by performing the ultrasonication at 130 kHz at a reduced power level for 1 to 2 h. The resulting films were heat treated in oxygen ambient at 530 °C for stoichiometric TiO₂ formation and crystallization.³³

The low magnification SEM images of a heat treated nanotube coated wire sample are shown in Figure 3A, and the high magnification images of the nanotubes are given in Figure 3B–D. The nanotube coating appeared like the bark of a tree (Figure 3A inset) with crevices formed between groups of nanotubes. Our studies show that the crevices were primarily formed during the growth of the nanotubes and not during heat treatment. The images in Figure S1 give a closer view of the rift between nanotubes. The nanotubes grown using ethylene glycol electrolyte in planar substrates have a more or less hexagonal close packed geometry.³¹ Such a configuration cannot be maintained in a cylindrical substrate geometry especially when the radius is small. The lateral stress across the nanotube film increases as the nanotube length increases, and as a result a partition is formed between nanotubes to relieve the stress. Our observation and conclusion are consistent with

those reported by Gulati et al.³⁸ who also observed cracks in their TNT films on wire substrates. Nonetheless, we note that the nanotubes were not detached from the substrate; rather, their alignment changed in the partition region. The nanotubes between the crevices were closely packed as evident from the side and top views of the nanotubes given in Figure 3B–D. The close packing is maintained from the bottom of the nanotube (Figure 3D inset) to the top. Nanotubes of length about 10 to 20 μm, pore diameter ~110 nm, and wall thickness ~20 nm (measured from SEM images) were used for the study.

In order to understand the structure and composition of the heat treated nanotubes on wire substrates, we performed HRTEM, GAXRD, and XPS studies. Figure 4a shows the HRTEM images of a nanotube mechanically separated from the wire substrate. The high resolution image of a nanotube region given in Figure 4b shows the polycrystalline lattice. The selected area diffraction pattern (SAD) from a few nanotubes (Figure 4c) revealed reflections from anatase phase of titania. GAXRD patterns obtained from a single nanotube coated wire (Figure S2) confirmed that the nanotubes consisted of anatase phase of titania. No other phase was found in the samples. This result was further substantiated by XPS studies. The XPS survey spectrum given in Figure 5 shows the peaks of titanium, oxygen, and carbon only. The high resolution scans of O 1s and Ti 2p peaks are given in the inset. The carbon peak is centered at ~288 eV, which can be attributed to C–O bonds. We believe that this peak arises from the carbon left on the surface after the burning of the organic electrolyte during heat treatment in oxygen ambient. We note that we did not estimate the stoichiometry of the nanotubes, as XPS does not provide the composition of nanoporous samples accurately.²⁶ Nonetheless, we do not expect any significant deviation from stoichiometry as the pristine oxide samples were heat treated in oxygen ambient. In short, the nanotubes are composed of pure titanium dioxide in anatase phase.

3.3. Phosphopeptide Separation Capacity Evaluation Using α -Casein. For the qualitative evaluation of phosphopeptide separation capacity of highly ordered TiO₂ nanotubes on

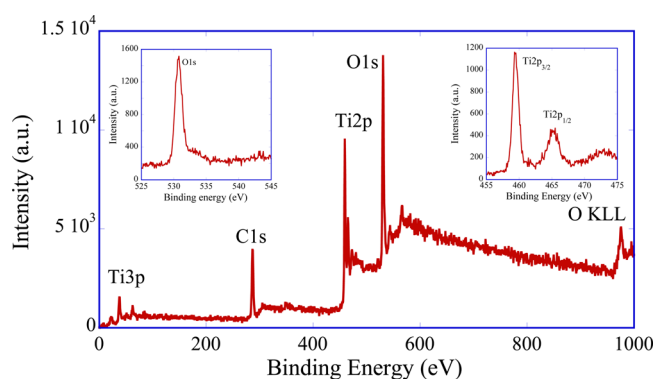


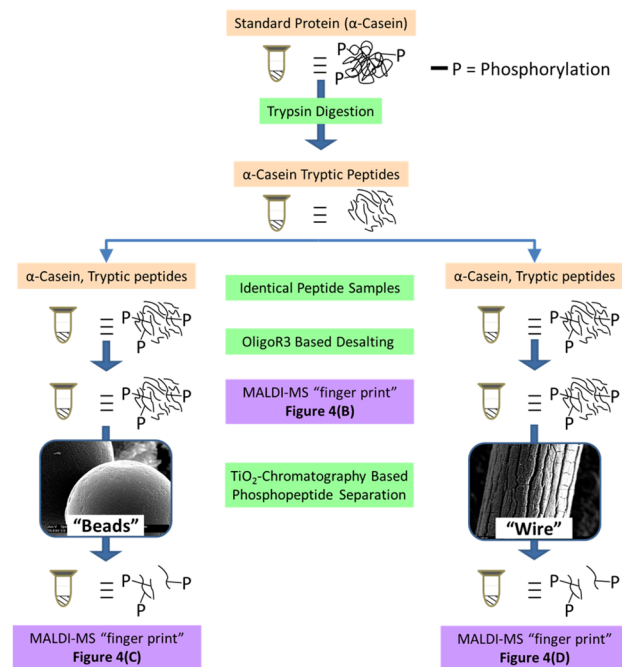
Figure 5. XPS survey spectrum from a titania nanotube film covered Ti wire. Inset: high resolution scans of the O 1s and Ti 2p peaks.

Ti-Metal “wires” prepared, phosphopeptide separation experiments were first performed using a standard phosphoprotein, α -casein. As illustrated in Figure 6A, tryptic digest from 500 μ g of α -casein was first separated into two identical aliquots, i.e., 250 μ g each, and subjected to OligoR3 based desalting as described in the methods. Prior to performing TiO_2 -chromatography, for comparison purposes, a MALDI-mass spectrum (or an MS “finger print”) was obtained for desalted α -casein tryptic digest (Figure 6B). During the TiO_2 -chromatography step, the desalted tryptic digests were pretreated with both “beads” and “wires”. After washing the captured

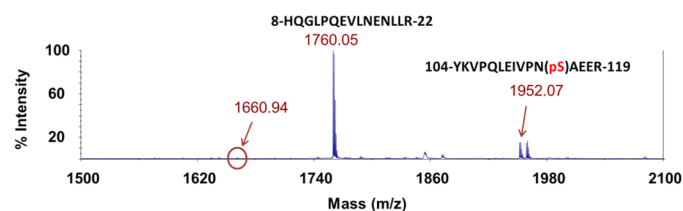
phosphopeptides and eluting them with ammonia solutions as described in methods, MALDI-mass spectra (or MS “finger-prints”) were obtained (Figure 6C,D). In analyzing the mass spectral regions (m/z 1500 to 2100), after performing TiO_2 -chromatography either using “beads” or “wires” on α -casein tryptic digests, the phosphopeptides, 106-VPQLEIVPN(pS)-AEER-119 and 104-YKVPQLEIVPN(pS)AEER-119 represented by m/z values at 1661.01 and 1952.20, are markedly abundant compared to before TiO_2 -treatment (compare Figure 6C,D). In Figure 6B, the most abundant peptide response for the α -casein tryptic peptide before TiO_2 -treatment is 8-HQGLPQEVLENLLR-22 (m/z 1760.05). The responses at m/z 1660.94 and 1952.07 are either infinitesimally small or relatively low in abundance, respectively. This qualitative illustration demonstrates that TiO_2 nanotubes, grown on pieces of Ti-metal wire, can be used to enrich phosphopeptides in a comparable manner to TiO_2 beads.

In real biological protein samples or proteomes, it is known that phosphorylation is substoichiometric or very low in abundance. Thus, separation of phosphopeptides from a cleaner/purified standard phosphoprotein digest sample is different from that of a digest that is derived from a tissue extract. Hence, to make these highly ordered TiO_2 nanotubes valuable, their capacity in phosphopeptide separation for studying complex phosphoproteomes derived from tissue extracts also needed to be evaluated and compared with

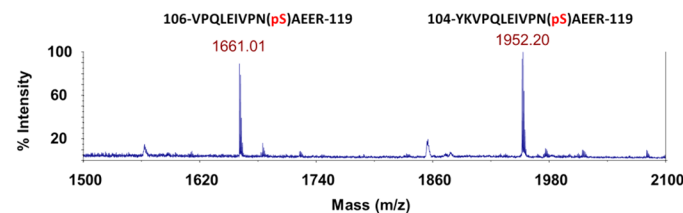
(A) Experimental Workflow



(B) MALDI-MS of α -Casein, Tryptic peptides



(C) MALDI-MS of α -Casein phosphopeptides—Separated by TiO_2 “beads”



(D) MALDI-MS of α -Casein phosphopeptides—Separated by TiO_2 “wires”

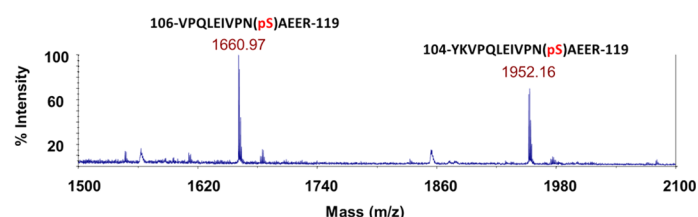


Figure 6. MALDI-MS analysis of tryptic peptides of phosphoprotein standard, α -casein, to compare phosphopeptide separation of Titansphere¹⁴ TiO_2 Bulk Material-beads and Ti-wire surface grown with TiO_2 nanotubes. (A) Experimental workflow— α -casein, 500 μ g was digested using trypsin. After desalting the samples using Oligo R3 beads, phosphopeptides were separated using TiO_2 -chromatography using identical amounts of α -casein tryptic peptides (250 μ g) using both Titansphere¹⁴ TiO_2 Bulk Material-beads (“Beads”) and Ti-wire pieces grown with TiO_2 nanotubes (“Wires”), as described elsewhere.⁹ (B) MALDI-mass spectrum of α -casein tryptic peptides, in m/z range 1500–2100, indicating the prominent peptide, 8-HQGLPQEVLENLLR-22 at m/z 1760.05; less prominent phosphorylated peptide, 104-YKVPQLEIVPN(pS)AEER-119 at m/z 1952.07; and infinitesimally small response for the phosphorylated peptide 106-VPQLEIVPN(pS)AEER-119 at m/z 1660.94. MALDI-mass spectrum of α -casein tryptic peptides, in m/z range 1500–2100, after phosphopeptide separation using (C) Titansphere¹⁴ TiO_2 Bulk Material-beads. (D) Ti-wire surface grown with TiO_2 nanotubes.

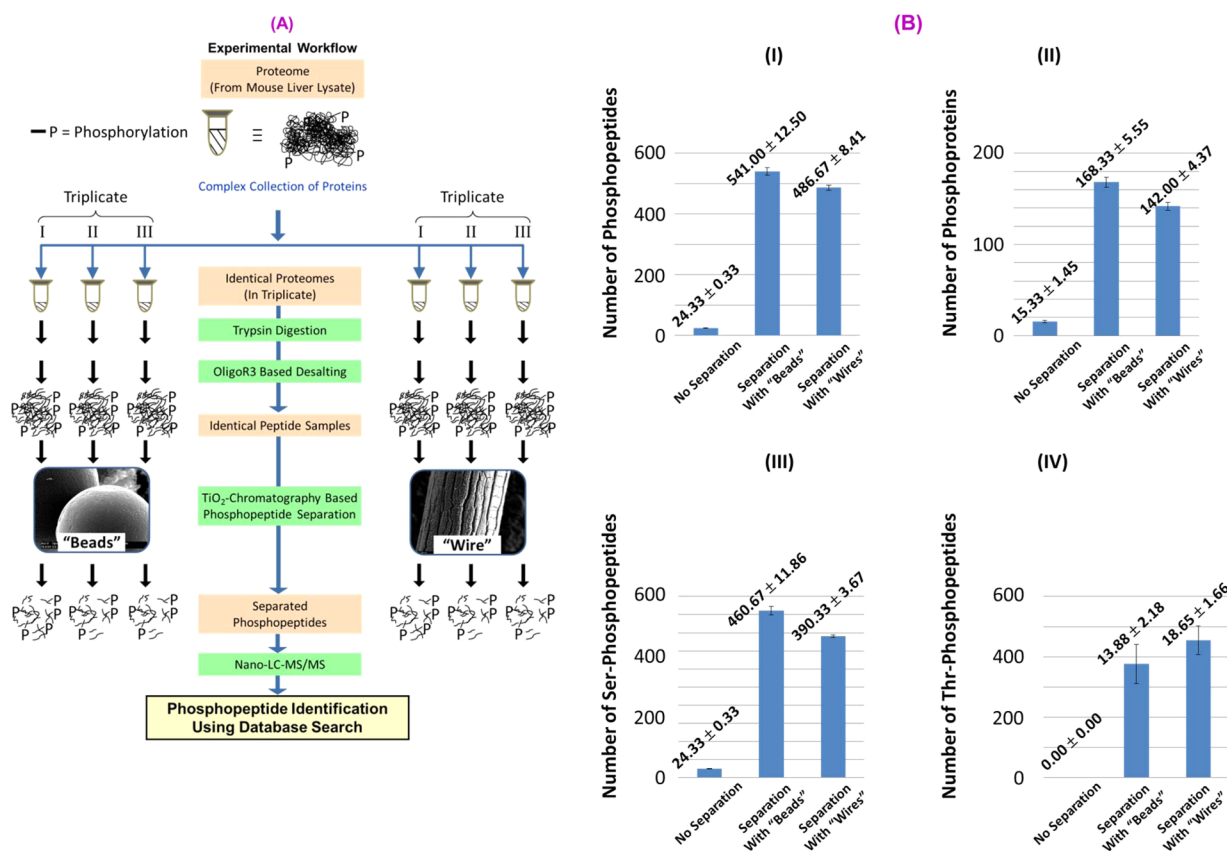


Figure 7. LC-MS/MS (liquid chromatography–mass spectrometry/tandem mass spectrometry) analysis and identification of mouse liver proteome tryptic peptides to compare phosphopeptide separation capacity of Titansphere¹⁴ TiO₂ Bulk Material-beads (“Beads”) and Ti-wire surface grown with TiO₂ nanotubes (“Wires”). (A) Experimental workflow: From a mouse liver lysate, six identical and 500 μg equivalent protein samples were digested with trypsin. After OligoR3 based desalting of the peptides, phosphopeptides were separated using TiO₂-chromatography using both Titansphere¹⁴ TiO₂ Bulk Material-beads (500 μg in mass) for three samples; and Ti-wire pieces grown with TiO₂ nanotubes (2 cm in length) for three samples, as described in the methods. Note: additionally, three 1 μg equivalent of tryptic digests from a mouse liver, with no phosphopeptide separation, were also analyzed using LC-MS/MS, so that “non-phosphopeptide separation” can be compared to phosphopeptide separation by either “beads” or “wire” TiO₂-chromatography methods. (B) Bar-graphs representing unique and high confidence (>95%): (I) average number of phosphopeptides; (II) respective average number of phosphoproteins; and (III) average number of Ser-phosphopeptides; (IV) average number of Thr-phosphopeptides.

respect to the widely used Titansphere TiO₂ Bulk Material-beads.

3.4. Phosphopeptide Separation Capacity Evaluation Using Complex Tissue Extracts. In order to examine the capability of TiO₂ nanotubes for phosphopeptide separation in proteomes of complex samples, we hypothesized that the number of high confidence (>95%) unique phosphopeptides identified using LC-MS/MS and database search algorithms is representative of the phosphopeptide separation capacity in a single phosphopeptide isolation. Hence, an experimental workflow, as depicted in Figure 7A, was implemented and analyzed for their unique phosphopeptide identifications. More specifically, from a single pool of mouse liver lysate, as described in the methods, six identical protein solutions (500 μg each) were sequentially subjected for protein precipitation, trypsin digestion, OligoR3 based desalting, and phosphopeptide separation using TiO₂-chromatography. In performing TiO₂-chromatography with “beads”, 500 μg equivalents of Titansphere TiO₂ Bulk Material-beads were used. For the “wires”, 2 cm (0.5 cm \times 4) of Ti-wire pieces grown with highly ordered TiO₂ nanotubes were used. The surface area of Titansphere TiO₂ Bulk Material-beads given by the manufacturer is 100 m²/g,¹⁸ and therefore, the surface area of 500 μg beads is about

0.05 m². The surface area of the nanotubes (pore diameter \sim 110 nm, wall thickness \sim 20 nm, and length about 15 μm) on a 2-cm-long wire of diameter 0.25 mm was calculated using the method reported elsewhere^{25,31} and is about 0.01 m². Thus, the Titansphere TiO beads used had surface area about 5 times the surface area of nanotubes. For comparison purposes, triplicate of 1 μg equivalent tryptic digests from mouse liver proteome were also analyzed using LC-MS/MS, so that “non-phosphopeptide separation” can be compared to phosphopeptide separation by either “beads” or “wire” based TiO₂-chromatography methods. It was assumed that 1 μg equivalent of tryptic digest analysis in LC-MS from a mouse liver could be used to illustrate the substoichiometric nature of phosphopeptides, and comparison of phosphopeptides identified in such an analysis is illustrative of the separation capacity in using either TiO₂-chromatography methodologies. Nevertheless, following all LC-MS/MS analyses/runs of each sample, as described in the methods, each LC-MS/MS run was subjected to database searches to identify high confidence (>95%) unique phosphopeptides. The confidence values were assigned for phosphopeptide identifications from the Paragon probabilistic algorithms used in ProteinPilot search software.

The average number of high confidence phosphopeptides (Paragon Plus algorithm assigned confidence >95%) identified and their average number of representative phosphoproteins were presented as bar-graphs, Figure 7B (I,II) for each “beads” and “wire” TiO₂-chromatography. In each graph represented in Figure 7, 1, “No Separation” represents the number of phosphopeptides identified in analyzing 1 μg equivalent of tryptic digest using LC-MS/MS with no TiO₂-chromatography performed; 2, “Separation with Beads”; and 3, “Separation with Wires” represent number of phosphopeptides identified in analyzing 500 μg equivalent of tryptic digest using LC-MS/MS with TiO₂-chromatography performed using Titansphere TiO₂ Bulk Material beads and Ti-wire surface grown with TiO₂ nanotubes, respectively. In inspecting Figures 7B (I,II), it is apparent that, although the surface area is lower, “wires” carry appreciable capacity (average number of phosphopeptides detected, 486.67 ± 8.41) to isolate phosphopeptides in reference to that observed when spherical “beads” are utilized (average number of phosphopeptides detected, 541.00 ± 12.50). In performing TiO₂-chromatography for phosphoproteomics studies, it has been well understood that phosphopeptides identified are phosphorylated mostly at serine (Ser or S) and then at threonine (Thr or T) amino acid residues. Thus, the average unique number of high confidence S-phosphopeptides and T-phosphopeptides identified were also plotted as bar-graphs (Figure 7B (III,IV)) for evaluation. It is evident that the “wires” carry a more or less similar capacity to isolate Ser-phosphorylated peptides (390.33 ± 3.67) and Thr-phosphorylated peptides (18.65 ± 1.66), compared to peptides identified with Ser-phosphorylation (460.67 ± 11.86) and Thr-phosphorylation (13.88 ± 2.18) when “beads” are employed. Overall, these results demonstrate that the highly ordered TiO₂ nanotube immobilization on Ti-metal wires carries significant potential as an alternate medium that can be utilized for mass spectrometry based phosphoproteomics workflows.

4. CONCLUSIONS

In this proof-of-concept study, we have evaluated the efficacy of titania nanotubes radially grown on titanium wire by anodic oxidation for phosphoproteomics. The data presented support the conclusion that this architecture can perform phosphopeptide enrichment with a similar capacity as commercially available Titansphere beads that are considered the most effective material for this purpose. Importantly, the nanotube dimensions can be further varied in length and diameter;²³ thus, one can likely precisely tune the parameters to further optimize their functionality. In addition, the nanotube-on-wire geometry facilitates the use of “length of the wire” as a way to easily assess the surface area for phosphopeptide separation experiments and thus eliminating the need for weighing precisely very small amounts of enrichment material or the variability associated with using slurry suspensions of material as in the case of beads. Furthermore, it may be possible to make the nanotube arrays available at a much lower cost than the present commercially available materials. In conclusion, we have demonstrated the TNTs on Ti wire offer similar efficacy for phosphopeptide enrichment compared to the current best approach, while at the same time offering an enhanced ease-of-use and the likelihood that further optimization in TNT length and/or diameter, will provide greater efficacy for phosphopeptide enrichment. Additional studies are ongoing to further enhance these new material for use in phosphoproteomics to the benefit of biomedical research.

■ ASSOCIATED CONTENT

Supporting Information

High resolution SEM images showing the cracks formed in the nanotube film on wire film and GAXRD pattern obtained from a single wire coated with nanotubes. The Supporting Information is available free of charge on the ACS Publications website at DOI: 10.1021/acsami.5b00799.

■ AUTHOR INFORMATION

Corresponding Authors

*E-mail: okvarghese@uh.edu. Phone: (1) 713 743-3808. Fax: (1) 713 743-3589.

*E-mail: ken.greis@uc.edu. Phone: (1) 513 558-7102. Fax: (1) 513 558 4454.

Author Contributions

A.W. and D.W. planned the experiments on phosphopeptide separation using titania nanotubes/beads and A.W. performed the experiments; M.P. planned the experiments on TiO₂ nanotube fabrication and imaged (SEM) the nanotubes; both M.P. and I.A. performed the nanotube fabrication; A.W., D.W., K.G., and O.V. composed the manuscript; K.G., O.V., and W.C. provided guidance and facilities for experiments; K.G. and O.V. edited the manuscript.

Notes

The authors declare no competing financial interest.

■ ACKNOWLEDGMENTS

This work was supported in part by funding by the University of Cincinnati Millennium Scholars Research Fund to K.D.G. and by the National Center for Research Resources S10 (RR027015) for shared instrumentation to K.D.G. O.K.V. acknowledges the financial support from University of Houston.

■ REFERENCES

- (1) Cohen, P. The Role of Protein Phosphorylation in Human Health and Disease. *Eur. J. Biochem.* **2001**, *268*, 5001–5010.
- (2) Eyrich, B.; Sickmann, A.; Zahedi, R. P. Catch Me if You can: Mass Spectrometry-based Phosphoproteomics and Quantification Strategies. *Proteomics* **2011**, *11*, 574–570.
- (3) Steen, H.; Mann, M. The ABC's (and XYZ's) of Peptide Sequencing. *Nat. Rev. Mol. Cell Biol.* **2004**, *5*, 699–711.
- (4) Steen, H.; Jebanathirajah, J. A.; Rush, J.; Morrice, N.; Kirschner, M. W. Phosphorylation Analysis by Mass Spectrometry: Myths, Facts, and the Consequences for Qualitative and Quantitative Measurements. *Mol. Cell. Proteomics* **2006**, *5*, 172–181.
- (5) Zou, Y.; Jiang, W.; Zou, L.; Li, X.; Liang, X. Ionization Suppression Effect of Phosphopeptides in Nano-electrospray Ionization Quadrupole Time-of-Flight Mass Spectrometry. *Chinese Journal of Chromatography* **2013**, *31*, 367–371.
- (6) Thingholm, T. E.; Jensen, O. N.; Larsen, M. R. Analytical Strategies for Phosphoproteomics. *Proteomics* **2009**, *9*, 1451–1468.
- (7) Dunn, J. D.; Reid, G. E.; Bruening, M. L. Techniques for Phosphopeptide Enrichment Prior to Analysis by Mass Spectrometry. *Mass Spectrom. Rev.* **2010**, *29*, 29–54.
- (8) Yan, Y.; Zheng, Z.; Deng, C.; Zhang, X.; Yang, P. Selective Enrichment of Phosphopeptides by Titania Nanoparticles Coated Magnetic Carbon Nanotubes. *Talanta* **2014**, *118*, 14–20.
- (9) Yan, Y.; Lu, J.; Deng, C.; Zhang, X. Facile Synthesis of Titania Nanoparticles Coated Carbon Nanotubes For Selective Enrichment of Phosphopeptides for Mass Spectrometry Analysis. *Talanta* **2013**, *107*, 30–35.
- (10) Najam-ul-Haq, M.; Jabeen, F.; Hussain, D.; Saeed, A.; Musharraf, S. G.; Huck, C. W.; Bonn, G. K. Versatile Nanocomposites in Phosphoproteomics: A Review. *Anal. Chim. Acta* **2012**, *747*, 7–18.

- (11) Fang, G.; Gao, W.; Deng, Q.; Qian, K.; Han, H.; Wang, S. Highly Selective Capture of Phosphopeptides Using a Nano Titanium Dioxide–multiwalled Carbon Nanotube Nanocomposite. *Anal. Biochem.* **2012**, *423*, 210–217.
- (12) Thingholm, T. E.; Jorgensen, T. J.; Jensen, O. N.; Larsen, M. R. Highly Selective Enrichment of Phosphorylated Peptides Using Titanium Dioxide. *Nat. Protoc.* **2006**, *1*, 1929–1935.
- (13) Jensen, S. S.; Larsen, M. R. Evaluation Of the Impact of Some Experimental Procedures on Different Phosphopeptide Enrichment Techniques. *Rapid Commun. Mass Spectrom.* **2007**, *15*, 3635–3645.
- (14) Larsen, M. R.; Thingholm, T. E.; Jensen, O. N.; Roepstorff, P.; Jørgensen, T. J. D. Selective Enrichment of Phosphorylated Peptides from Peptide Mixtures Using Titanium Dioxide Microcolumns. *Mol. Cell. Proteomics* **2005**, *4*, 873–886.
- (15) Liang, S. S.; Makamba, H.; Huang, S. Y.; Chen, S. H. Nano-Titanium Dioxide Composites for the Enrichment of Phosphopeptides. *J. Chromatogr., A* **2006**, *1116*, 38–45.
- (16) Wijeratne, A. B.; Manning, J. R.; Schultz, J. J.; Greis, K. D. Quantitative Phosphoproteomics Using Acetone-Based Peptide Labeling: Method Evaluation and Application to a Cardiac Ischemia/Reperfusion. *J. Proteome Res.* **2013**, *12*, 4268–4279.
- (17) Thingholm, T. E.; Jensen, O. N.; Robinson, P. J.; Larsen, M. R. SIMAC (Sequential Elution from IMAC), a Phosphoproteomics Strategy for the Rapid Separation of Monophosphorylated from Multiply Phosphorylated Peptides. *Mol. Cell. Proteomics* **2008**, *7*, 661–671.
- (18) GL Sciences; <http://www.glsciences.com/c-product/phosphopeptides/titansphere-tio-bulk-material/> (accessed November 21, 2013).
- (19) Li, Q. R.; Ning, Z. B.; Tang, J. S.; Nie, S.; Zeng, R. Effect of Peptide-to-TiO₂ Beads Ratio on Phosphopeptide Enrichment Selectivity. *J. Proteome Res.* **2009**, *8*, 5375–5381.
- (20) Gong, D.; Grimes, C. A.; Varghese, O. K.; Chen, Z.; Dickey, E. C. Titanium Oxide Nanotube Arrays Prepared by Anodic Oxidation. *J. Mater. Res.* **2001**, *16*, 333–3334.
- (21) Zwilling, V.; Darque-Ceretti, E.; Boutry-Forveille, A.; David, D.; Perrin, M. Y.; Aucouturier, M. Structure and Physicochemistry of Anodic Oxide Films on Titanium and TA6V Alloy. *Surf. Interface Anal.* **1999**, *27*, 629–637.
- (22) Richter, C.; Panaitescu, E.; Wiley, R.; Menon, L. Titania Nanotubes Prepared by Anodization in Fluorine-Free Acids. *J. Mater. Res.* **2007**, *22*, 1624–1631.
- (23) Rani, S.; Roy, S. C.; Paulose, M.; Varghese, O. K.; Mor, G. K.; Kim, S.; Yoriya, S.; LaTempa, T. J.; Grimes, C. A. Synthesis and Applications of Electrochemically Self-assembled Titania Nanotube Arrays. *Phys. Chem. Chem. Phys.* **2010**, *12*, 2780–2800.
- (24) Roy, P.; Berger, S.; Schmuki, P. TiO₂ Nanotubes: Synthesis and Applications. *Angew. Chem., Int. Ed.* **2011**, *50*, 2904–2939.
- (25) Varghese, O. K.; Paulose, M.; Grimes, C. A. Long Vertically Aligned Titania Nanotubes on Transparent Conducting Oxide for Highly Efficient Solar Cells. *Nat. Nanotechnol.* **2009**, *4*, 592–597.
- (26) Varghese, O. K.; Paulose, M.; LaTempa, T. J.; Grimes, C. A. High-Rate Solar Photocatalytic Conversion of CO₂ and Water Vapor to Hydrocarbon Fuels. *Nano Lett.* **2009**, *9*, 731–737.
- (27) Kar, A.; Raja, K. S.; Misra, M. Electrodeposition of Hydroxyapatite onto Nanotubular TiO₂ for Implant Applications. *Surf. Coat. Technol.* **2006**, *201*, 3723–3731.
- (28) Lo, C.-Y.; Lin, J.-Y.; Chen, W.-Y.; Chen, C.-T.; Chen, Y.-C. Surface-Assisted Laser Desorption/Ionization Mass Spectrometry on Titania Nanotube Arrays. *J. Am. Soc. Mass Spectrom.* **2008**, *19*, 1014–1020.
- (29) Min, Q.; Chen, X.; Zhang, X.; Zhu, J.-J. Tailoring of a TiO₂ Nanotube Array-Integrated Portable Microdevice for Efficient On-Chip Enrichment and Isotope Labeling of Serum Phosphopeptides. *Lab Chip* **2013**, *13*, 3853–3861.
- (30) Paulose, M.; Shankar, K.; Yoriya, S.; Prakasham, H. E.; Varghese, O. K.; Mor, G. K.; LaTempa, T. A.; Fitzeral, A.; Grimes, C. A. Anodic Growth of Highly Ordered TiO₂ Nanotube Arrays to 134 Micron in Length. *J. Phys. Chem. B* **2006**, *110*, 16179–16184.
- (31) Shankar, K.; Mor, G. K.; Prakasham, H. E.; Yoriya, S.; Paulose, M.; Varghese, O. K.; Grimes, C. A. Highly-Ordered TiO₂ Nanotube Arrays up to 220 μm in Length: Use in Water Photoelectrolysis and Dye-Sensitized Solar Cells. *Nanotechnology* **2007**, *18*, 065707.
- (32) Jarrold, B.; DeMuth, J.; Greis, K.; Burt, T.; Wang, F. An Effective Skeletal Muscle Prefractionation Method to Remove Abundant Structural Proteins for Optimized Two-Dimensional Gel Electrophoresis. *Electrophoresis* **2005**, *26*, 2269–2278.
- (33) Varghese, O. K.; Gong, D.; Paulose, M.; Grimes, C. A.; Dickey, E. C. Crystallization and High-temperature Structural Stability of Titanium Oxide Nanotube Arrays. *J. Mater. Res.* **2003**, *18*, 156–165.
- (34) Eriksson, A. I. K.; Edwards, K.; Hagfeldt, A.; Hernández, V. A. Physicochemical Characterization of Phosphopeptide/Titanium Dioxide Interactions Employing the Quartz Crystal Microbalance Technique. *J. Phys. Chem. B* **2013**, *117*, 2019–2025.
- (35) Connor, P. A.; McQuillan, A. J. Phosphate Adsorption onto TiO₂ from Aqueous Solutions: An In Situ Internal Reflection Infrared Spectroscopic Study. *Langmuir* **1999**, *15*, 2916–2921.
- (36) Engholm-Keller, K.; Larsen, M. R. Titanium Dioxide as Chemo-Affinity Chromatographic Sorbent of Biomolecular Compounds Applications in Acidic Modification-Specific Proteomics. *J. Proteomics* **2011**, *75*, 317–328.
- (37) Paulose, M.; Prakasham, H. E.; Varghese, O. K.; Peng, L.; Popat, K. C.; Mor, G. K.; Desai, T. A.; Grimes, C. A. TiO₂ Nanotube Arrays of 1000 μm Length by Anodization of Titanium Foil: Phenol Red Diffusion. *J. Phys. Chem. C* **2007**, *111*, 14992.
- (38) Gulati, K.; Aw, M. S.; Losic, D. Nanoengineered Drug-releasing Ti Wire as an Alternative for Local Delivery of Chemotherapeutics in the Brain. *Int. J. Nanomed.* **2012**, *7*, 2069–2076.
- (39) Tao, J.; Zhao, J.; Wang, X.; Kang, Y.; Li, Y. Fabrication of Titania Nanotube Arrays on Curved Surface. *Electrochem. Commun.* **2008**, *10*, 1161–1163.
- (40) Garcia-Vergara, S. J.; Skeldon, P.; Thompson, G. E.; Habazaki, H. A Flow Model of Porous Anodic Film Growth on Aluminium. *Electrochim. Acta* **2006**, *52*, 681–687.